

A review of the mobile LIDAR system developed at the CSIR and a proposed improvement of the system

ABSTRACT

We report on the mobile LIDAR system developed at the CSIR-National Laser Centre. We show some measurements that have been done with this system. We also show the alterations planned to improve the system.

INTRODUCTION

LIDAR is an acronym for light detection and ranging, it is analogous to radar (radio detection and ranging), except that it is based on discrete light pulses and measured travel times. The advancement in both laser and detector technology along with improvements in data-acquisition and analysis techniques have made lidar a very reliable tool for active atmospheric remote sensing [1]. With this advancement a lidar system can be employed to measure: (1) temperature (structure from ground to thermosphere, diurnal/seasonal/interannual variations, etc.), (2) Wind (structure from ground to upper atmosphere, its variations, etc.), (3) Aerosols and clouds (distribution, extinction, composition, size, shape, and variations spatially and temporally), (4) Constituents (O_3 , CO_2 , H_2O , O_2 , N_2^+ , He, metal atoms like Na, Fe, K, Ca, pollution, etc.) and (5) Target & altimetry (identification, accurate height & range determination, fish, vibration, etc.).

It has been discovered that there is more water content in the upper reaches of the troposphere than was previously thought to exist. Water vapour absorbs infrared radiation emitted from earth's surface and lower atmosphere more than any other constituent, thereby trapping heat best. This makes water vapour the worst candidate contributing to global warming. Therefore high-altitude water-vapour measurement is a key element in modelling global warming because water has a much greater influence on earth's tropospheric energy balance than trace gases such as carbon dioxide. Water vapour is also one of the least understood and poorly described components of the earth's atmosphere. LIDAR is a tool that can be used to study this.

CURRENT LIDAR SYSTEM

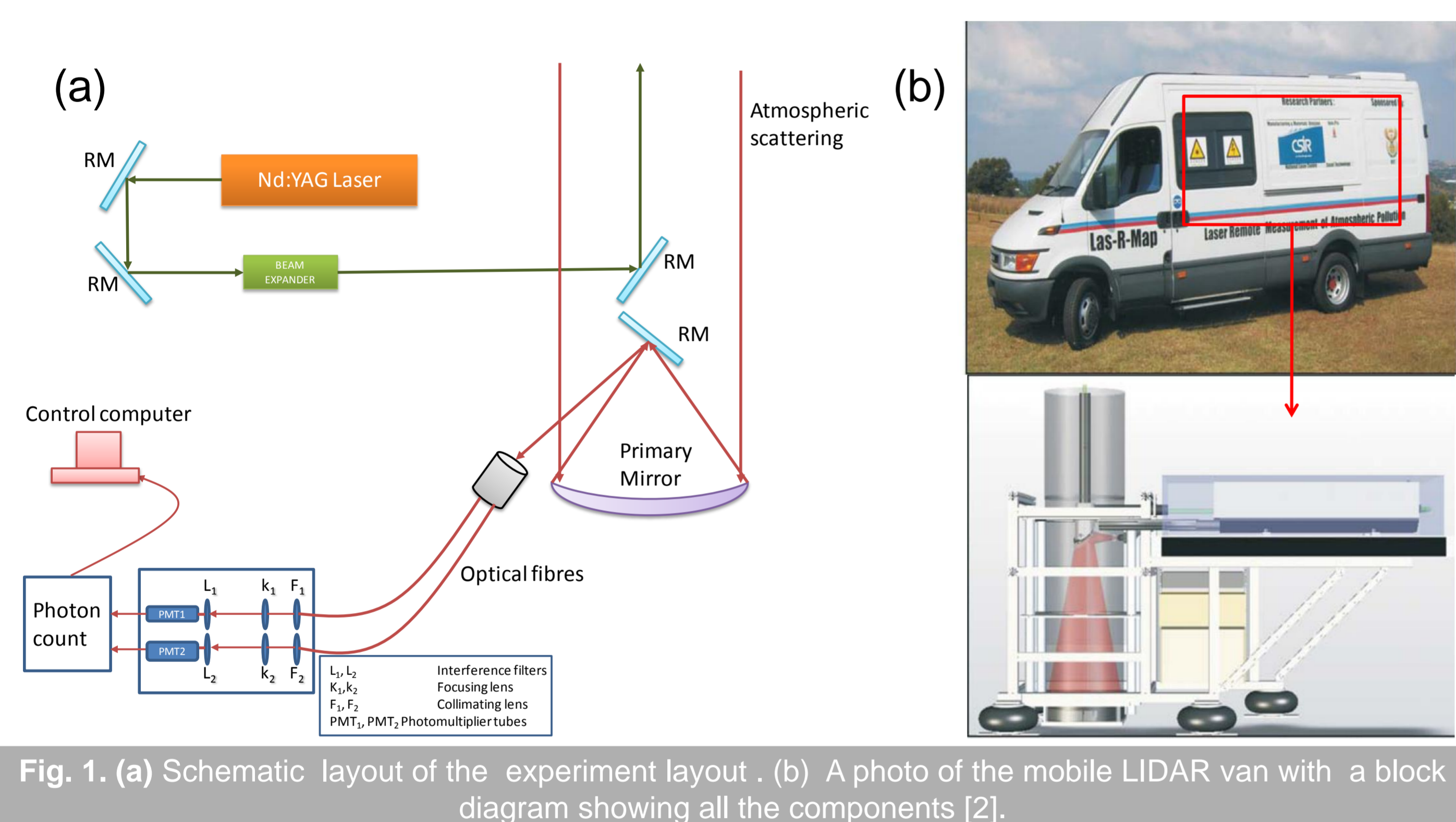


Fig. 1. (a) Schematic layout of the experiment layout. (b) A photo of the mobile LIDAR van with a block diagram showing all the components [2].

In the case of a Raman lidar system (inelastic scattering) the backscattered power at wavelength that has been shifted from the laser wavelength due to inelastic Raman scattering by molecular species X, is given by the following expression [3]:

$$P(\lambda_s, r) = P(\lambda_e) O(r) \frac{A}{r^2} C(\lambda_s, r) \beta(\lambda_s, \lambda_e) \exp\left[-\int_0^r (\alpha(\lambda_s, r) + \alpha(\lambda_e, r)) dr\right] + P_n \quad (1)$$

$P(\lambda_e)$ is the emitted power at laser wavelength, $O(r)$ is the overlap function, A is the area of the telescope, $C(\lambda_s, r)$ is a system constant accounting for the transmission of the receiver unit, $\beta(\lambda_s, \lambda_e)$ the backscatter coefficients, $\alpha(\lambda_s, r)$ and $\alpha(\lambda_e, r)$ are the extinction coefficient, and P_n is the background power (straylight or detector noise).

Backscatter signals are measured at two different wavelengths in the rotational Raman spectrum and the temperature can be estimated from the ratio of these two signals as follows [3]:

$$T(r) = \frac{A}{\log\left[\frac{P(\lambda_{s1}, r) - P_{n1}}{P(\lambda_{s2}, r) - P_{n2}}\right]} + B \quad (2)$$

where, A and B are calibration constants, that are derived from intercomparisons external measurements.

Relative humidity was retrieved from the aerosol backscatter co-efficient, using the relation between the relative humidity Rh and backscattering co-efficients β described as [4],

$$\left(\frac{\beta(\lambda_s, r)}{\beta_{70}(\lambda_s, r)}\right) = a \left(1 - \frac{Rh}{100}\right)^b \quad (3)$$

where $\beta_{70}(\lambda_s, r)$ is taken at a relative humidity Rh value of 70 %, noted from the Irene Balloon borne measurements.

Table 1. Major specifications of the LIDAR system. The transmitter and receiver are co-located, resulting in a monostatic configuration that maximises the overlap of the outgoing beam with the receiver field of view [2].

Transmitter		Signal and data processing		Receiver		Personal Computer	
Parameters	Specifications	Parameters	Specifications	Parameters	Specifications	Parameters	Specifications
Laser source	Nd:YAG-Continuum®	Model	Lico®TR15-40	Telescope type	Newtonian	TR-40 interface	Ethernet
Operating wavelength	532nm	Memory depth	4096	Diameter	404mm	Processor	Intel®CoreDuo 2.6 GHz
Average pulse energy	150mJ (@532nm)	Maximum range	40.96 km	Field of view	0.5 mrad	Operating system	Windows®XP Pro
Beam expander	3x	Spatial resolution	10m	PMT	Hananatsu® R7400-U20	Software interface	NI LabView®
Pulse width	7ns			Optical fibre	Multimode, 600 µm core		
Pulse repetition	10Hz			Field FWHM	0.7mm		
Beam divergence	0.2 mrad after beam expander						

L. Shikwambana^{1,2}, V. Sivakumar¹ AND A. Sharma²
¹School of Physics, University of KwaZulu-Natal, Private Bag X54001, Durban 4000, South Africa
²CSIR National Laser Centre, PO Box 395, Pretoria 0001, South Africa
 Email: lshikwambana@csir.co.za - www.csir.co.za

EXPERIMENTAL RESULTS

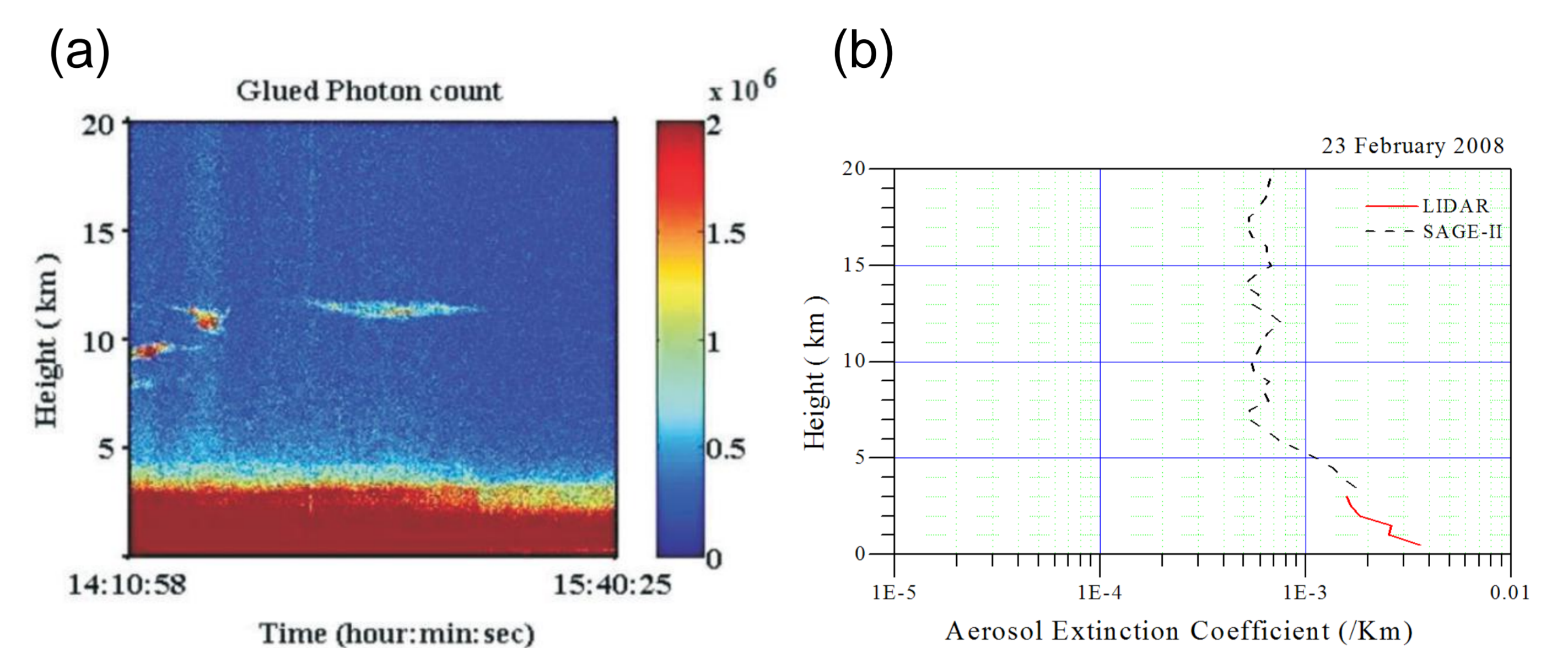


Fig. 2 (a) Height-time-colour map of LIDAR signal returns for 25 February 2008 [5]. (b) Height profile of aerosol extinction derived from LIDAR signal returns and SAGE-II satellite data [6].

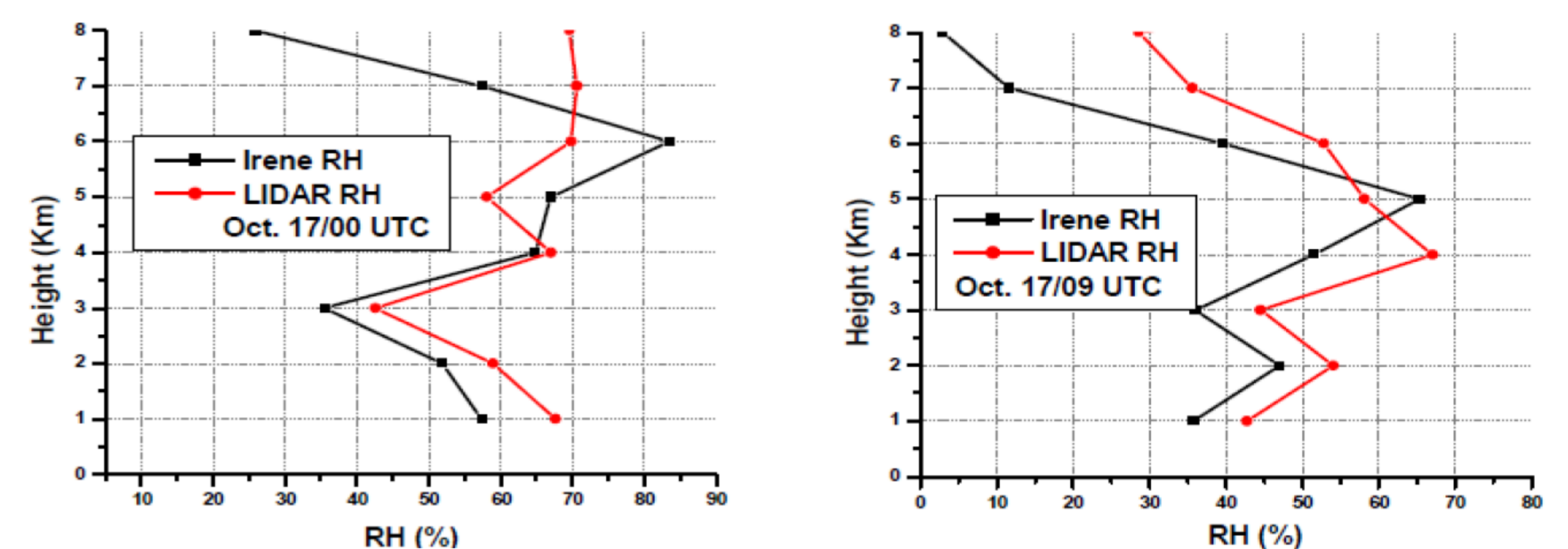


Fig. 3. Height profile of relative humidity derived from LIDAR aerosol backscatter co-efficient and the radiosonde measured [4].

PROPOSED MODIFICATIONS OF THE LIDAR SYSTEM

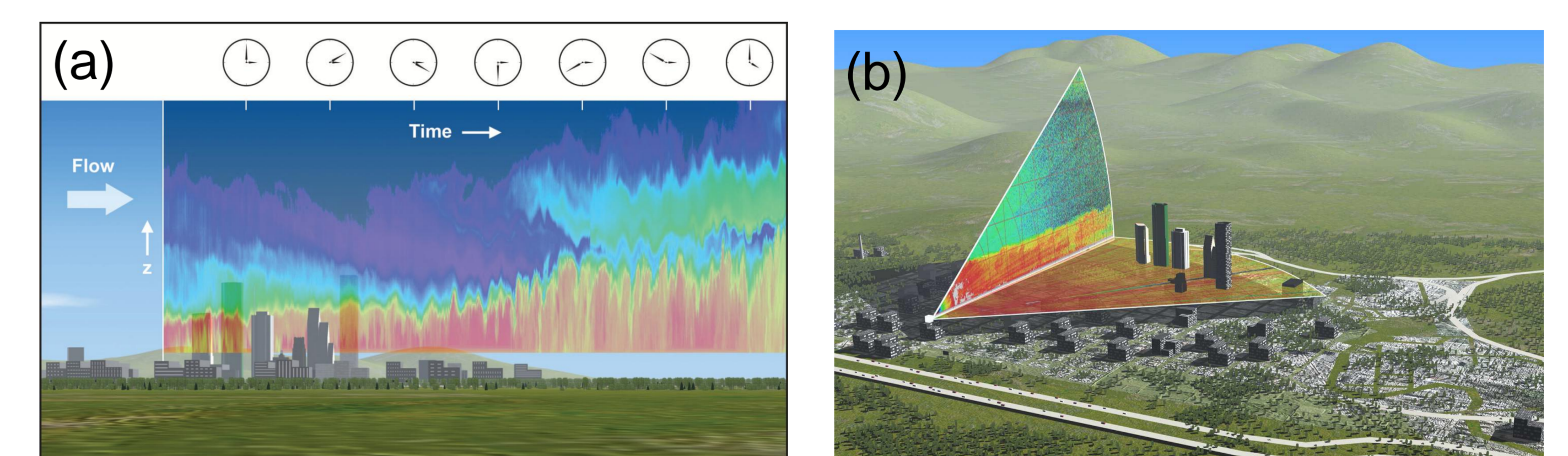


Fig. 4. (a) Ground-based zenith-pointing lidars are limited to providing time history versus altitude data. (b) Ground-based scanning lidars can provide data on both horizontal and vertical planes. The two different scans can be interleaved sequentially in order to provide both horizontal and vertical animations over the same time period.

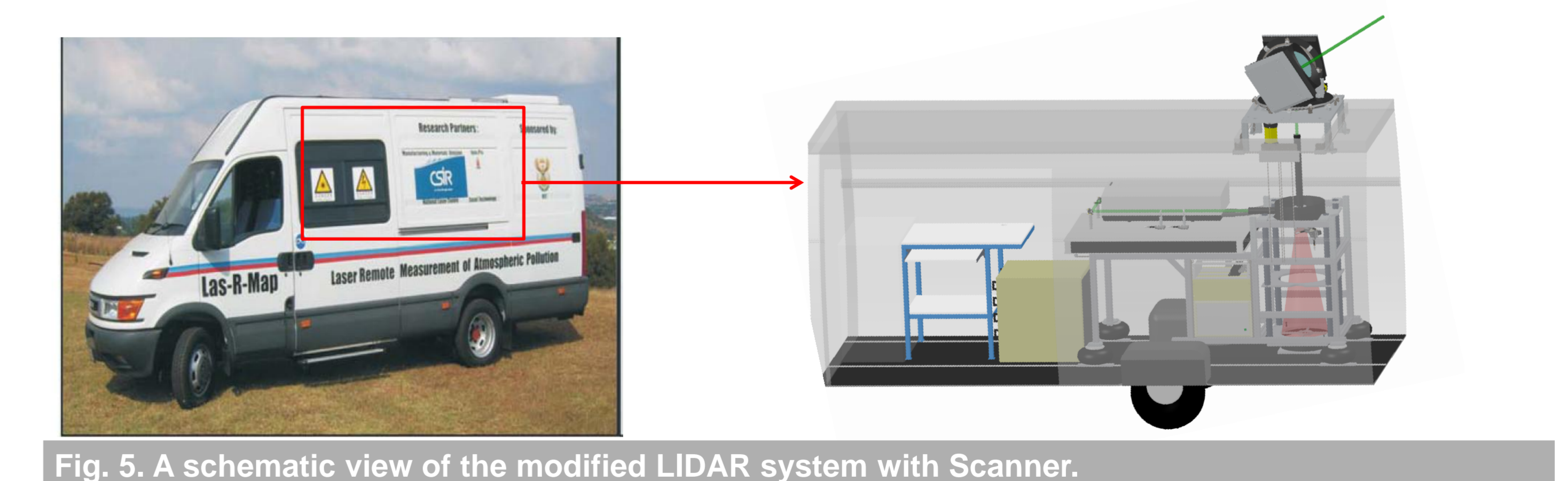


Fig. 5. A schematic view of the modified LIDAR system with Scanner.

The integration of a scanner into the present LIDAR system will be implemented by a cable/pulley system and an electric winch to lift and lower the scanner. The integration of the scanner will assist us in terms of (1) X-Y dimensional mapping of the atmosphere (horizontal or vertical cross-section), (2) Focusing the target (industrial smoke or cloud of pollutants) and (3) To study the plume (say smoke, biomass burning and etc), Haze and Aerosol/pollutant dispersion.

REFERENCES

- [1] V. Sivakumara (2008), Lidar research in South Africa, *SPIE Newsroom*, 10.1117/2.1200808.1250.
- [2] A. Sharma, V. Sivakumara, C. Bollig, C. van der Westhuizen and D. Moema (2009), System description of the mobile LIDAR of the CSIR, South Africa, *South African Journal of Science*, no. 105, pp. 456-462.
- [3] http://wiki.eg-climet.org/index.php?title=Raman_LIDAR_Fundamentals.
- [4] M. Tesfaye, V. Sivakumar, J. Botai, D. Moema, A. Sharma, C. Bollig, C.J. deW. Hannes Rautenbach and G. Mengistu (2009), Retrieval of relative humidity from CSIR-NLC mobile lidar backscatter measurements, *SASAS conference proceeding*, pp. 8-9.
- [5] V. Sivakumara, M. Tesfaye, W. Alemu, D. Moema, A. Sharma, C. Bollig and G. Mengistu (2009), CSIR South Africa mobile LIDAR—First scientific results: comparison with satellite, sun photometer and model simulations, *South African Journal of Science*, no. 105, pp. 449-455.
- [6] V. Sivakumara, M. Tesfaye, W. Alemu, A. Sharma and C. Bollig (2008), AEROSOL MEASUREMENTS OVER SOUTH AFRICA USING SATELLITE, SUN-PHOTOMETER AND LIDAR, *Advances in Geosciences; volume 16: Atmospheric Science*, pp. 253-262.